

AD 739498

# Photoemission from Polymers

Prepared by F. HAI and M. J. BERNSTEIN  
Plasma Research Laboratory

72 MAR 15

Reproduced by  
NATIONAL TECHNICAL  
INFORMATION SERVICE  
Springfield, Va. 22151

---

Laboratory Operations  
THE AEROSPACE CORPORATION

---

Prepared for SPACE AND MISSILE SYSTEMS ORGANIZATION  
AIR FORCE SYSTEMS COMMAND  
LOS ANGELES AIR FORCE STATION  
Los Angeles, California

APPROVED FOR PUBLIC RELEASE;  
DISTRIBUTION UNLIMITED

D D C  
RECEIVED  
APR 3 1972  
RECEIVED  
D 29

CSSTI	WHITE SECTION	<input checked="" type="checkbox"/>
DBB	BUFF SECTION	<input type="checkbox"/>
UNAL. CED.		<input type="checkbox"/>
JUSTIFICATION		
BY		
DISTRIBUTION/AVAILABILITY CODES		
DIST.	AVAIL. and/or	SPECIAL
A		

## LABORATORY OPERATIONS

The Laboratory Operations of The Aerospace Corporation is conducting experimental and theoretical investigations necessary for the evaluation and application of scientific advances to new military concepts and systems. Versatility and flexibility have been developed to a high degree by the laboratory personnel in dealing with the many problems encountered in the nation's rapidly developing space and missile systems. Expertise in the latest scientific developments is vital to the accomplishment of tasks related to these problems. The laboratories that contribute to this research are:

Aerodynamics and Propulsion Research Laboratory: Launch and reentry aerodynamics, heat transfer, reentry physics, propulsion, high-temperature chemistry and chemical kinetics, structural mechanics, flight dynamics, atmospheric pollution, and high-power gas lasers.

Electronics Research Laboratory: Generation, transmission, detection, and processing of electromagnetic radiation in the terrestrial and space environments, with emphasis on the millimeter-wave, infrared, and visible portions of the spectrum; design and fabrication of antennas, complex optical systems and photolithographic solid-state devices; test and development of practical superconducting detectors and laser devices and technology, including high-power lasers, atmospheric pollution, and biomedical problems.

Materials Sciences Laboratory: Development of new materials; metal matrix composites and new forms of carbon; test and evaluation of graphite and ceramics in reentry; spacecraft materials and components in radiation and high-vacuum environments, application of fracture mechanics to stress corrosion and fatigue-induced fractures in structural metals, effect of nature of material surfaces on lubrication, photosensitization, and catalytic reactions, and development of prosthesis devices.

Plasma Research Laboratory: Reentry physics and nuclear weapons effects; the interaction of antennas with reentry plasma sheaths, experimentation with thermonuclear plasmas, the generation and propagation of plasma waves in the magnetosphere, chemical reactions of vibrationally excited species in rocket plumes; and high-precision laser ranging.

Space Physics Laboratory: Aeronomy, density and composition of the atmosphere at all altitudes, atmospheric reactions and atmospheric optics; pollution of the environment; the sun, earth's resources, meteorological measurements, radiation belts and cosmic rays, and the effects of nuclear explosions, magnetic storms, and solar radiation on the atmosphere.

THE AEROSPACE CORPORATION  
El Segundo, California

UNCLASSIFIED  
Security Classification

DOCUMENT CONTROL DATA - R & D		
(Security classification of title, body of abstract and indexing annotation must be entered when the overall report is classified)		
1 ORIGINATING ACTIVITY (Corporate author)  The Aerospace Corporation El Segundo, California		2a REPORT SECURITY CLASSIFICATION Unclassified  2b GROUP
3. REPORT TITLE  PHOTOEMISSION FROM POLYMERS		
4 DESCRIPTIVE NOTES (Type of report and inclusive dates)		
5 AUTHOR(S) (First name, middle initial, last name)  Francis Hai and Melvin J. Bernstein		
6 REPORT DATE 72 MAR 15	7a TOTAL NO. OF PAGES 24	7b NO OF REFS 10
8a CONTRACT OR GRANT NO F04701-71-C-0172  b PROJECT NO	9a ORIGINATOR'S REPORT NUMBER(S) TR-0172(2220-60)-2  9b OTHER REPORT NO(S) (Any other numbers that may be assigned this report) SAMSO-TR-72-26	
10 DISTRIBUTION STATEMENT  Approved for public release; distribution unlimited		
11 SUPPLEMENTARY NOTES	12 SPONSORING MILITARY ACTIVITY Space and Missile Systems Organization Air Force Systems Command Los Angeles, California	
13 ABSTRACT  An experimental study has been made of photoemission from several polymers, including polyethylene, kapton, teflon, and polyvinyl chloride, under irradiation by 15 to 25 keV photons. The emission intensities from these plastics were compared to those from several conductors, ranging from carbon to tantalum, and from other insulators such as glass and mica. For all these materials, the relative magnitude of photoemission was found to be mainly proportional to the photoelectric absorption coefficient. Under this pulsed irradiation, the insulators emitted as conductors when backed by conducting sheets but exhibited reduced emission associated with trapped charges when isolated.		

UNCLASSIFIED

Security Classification

14

KEY WORDS

Photoelectron Emission  
Polymers  
Secondary Electron Emission

Distribution Statement (Continued)

Abstract (Continued)

UNCLASSIFIED

Security Classification

Air Force Report No.  
SAMSO-TR-72-26

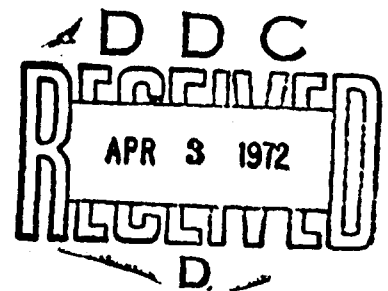
Aerospace Report No.  
TR-0172(2220-60)-2

PHOTOEMISSION FROM POLYMERS

Prepared by  
F. Hai and M. J. Bernstein  
Plasma Research Laboratory

72 MAR 15

Laboratory Operations  
THE AEROSPACE CORPORATION



Prepared for  
SPACE AND MISSILE SYSTEMS ORGANIZATION  
AIR FORCE SYSTEMS COMMAND  
LOS ANGELES AIR FORCE STATION  
Los Angeles, California

Approved for public release;  
distribution unlimited

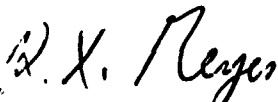
## FOREWORD

This report is published by The Aerospace Corporation, El Segundo, California, under Air Force Contract No. F04701-71-C-0172.

This report, which documents research carried out from November 1970 to June 1971, was submitted 4 January 1972 to Captain Karl J. Hoch, SYAE, for review and approval.

The authors are indebted to G. G. Comisar for many helpful discussions, to V. Josephson for suggesting these measurements, to H. L. van Paassen and R. H. Vandre for determination of the photon spectrum, and to R. L. Walter for assistance in performing the experiments.

Approved



---

R. X. Meyer, Director  
Plasma Research Laboratory

Publication of this report does not constitute Air Force approval of the report's findings or conclusions. It is published only for the exchange and stimulation of ideas.



---

Karl J. Hoch  
Capt., United States Air Force  
Project Officer

# ABSTRACT

An experimental study has been made of photoemission from several polymers, including polyethylene, kapton, teflon, and polyvinyl chloride, under irradiation by 15 to 25 keV photons. The emission intensities from these plastics were compared to those from several conductors, ranging from carbon to tantalum, and from other insulators such as glass and mica. For all these materials, the relative magnitude of photoemission was found to be mainly proportional to the photoelectric absorption coefficient. Under this pulsed irradiation, the insulators emitted as conductors when backed by conducting sheets but exhibited reduced emission associated with trapped charges when isolated.

## CONTENTS

FOREWORD . . . . .	ii
ABSTRACT . . . . .	iii
I. INTRODUCTION . . . . .	1
II. EXPERIMENT . . . . .	3
III. ANALYSIS . . . . .	11
IV. DISCUSSION AND CONCLUSION . . . . .	19
REFERENCES . . . . .	23

## FIGURES

1. Total Energy Flux Spectrum Incident on Diodes as Determined by Ross Filter Measurements . . . . .	2
2. Diagram of the Parallel Diodes . . . . .	4
3. Ratio of Biased Diode Signal to Unbiased Diode Signal as a Function of Bias Voltage for PVC and Aluminum . . . . .	7
4. Variation of Normalized Photoemission with the Mass Absorption Coefficient at 22 keV for Various Materials . . . . .	8
5. Emission Signals from PVC Observed on the Diode Collectors . . . . .	10
6. Variation of Electron Range with Electron Energy . . . . .	13

## TABLES

1. Parameters in Photoemission from Polymers and Other Materials . . . . .	5
2. Biased Diode Parameters . . . . .	15



## I. INTRODUCTION

Radiation-induced electron emission from solids is of direct interest in such problems as generation of replacement currents, production of transient electromagnetic fields, and charging of dielectric materials. This photoemission from metals has been experimentally examined (Ref. 1), and correlation with theory has been observed (Ref. 2). The objectives of the present investigation are to measure the emission from several polymers and to determine whether the theory that describes emission from metals also describes that from polymers.

The intense pulsed radiation source used in this investigation was a plasma focus discharge (Ref. 3). Ross filter measurements of the emitted radiation, shown in Fig. 1, indicate that the photon energies were mostly in the range from approximately 15 to 25 keV. Absorption measurements show exponential attenuation characteristic of 22 keV photons. This spectrum results mainly from K line radiation produced by the silver anode tip used in this device.

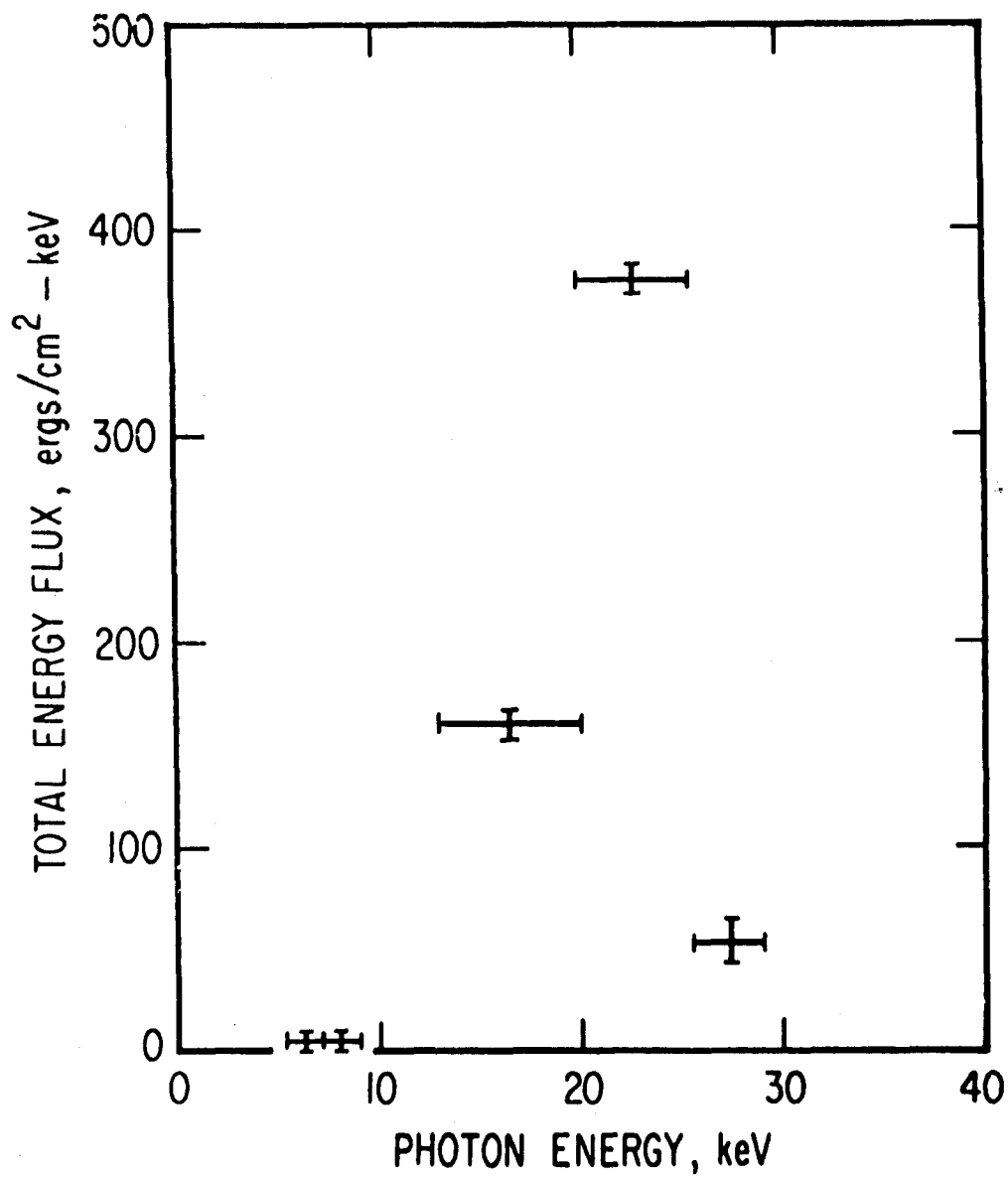


Figure 1. Total Energy Flux Spectrum Incident on Diodes as Determined by Ross Filter Measurements

Flux above 30 keV was less than 20 ergs/cm²-keV.

## II. EXPERIMENT

The experimental arrangement used in the measurement of photoemission is shown in Fig. 2. Photons from the plasma focus discharge impinged on two parallel diode structures. One diode with an aluminum emitter served as reference, and its emission signal was used for normalization because the fluence level varied from discharge to discharge. The other diode was used to measure the emissions from the various materials listed in Table 1. Only commercially available samples were examined; these varied widely with respect to sheet thickness. The same fluence and spectrum were obtained at the emitting surfaces of both the test and reference diodes by placing identical but reordered samples in each of the diodes, as indicated in Fig. 2. Also, the same fluence and spectrum were obtained for all the samples by adding sheets of aluminum to the thin samples such that the total exponential photon attenuation was about the same as that for the thick samples.

In the quantitative measurements of the relative emissions, the polymers and the other insulators were backed by grounded aluminum sheets; the reference aluminum emitter was also directly grounded. The emission areas in the two diodes were defined by two 2.86 cm diam holes cut in a lead collimator 1 cm in thickness. The collector in each diode was a 0.075 cm sheet of graphite backed by lead, 1 cm in thickness, and all extraneous surfaces were coated with carbon (Aquadag) to minimize electron emission. A sheet of mylar directly separated the two emission regions. The time-varying emission current in each diode was determined by the voltage drop across a 50-ohm resistor terminating the collector lead to ground; this signal was recorded on a Tektronix 555 oscilloscope. In addition, the radiation pulse was monitored simultaneously by a PIN silicon x-ray detector. Aluminum emitters were placed in the two diodes in order to check the equivalence of emission from both. The observed signals showed that the pulse shapes of the two emissions were identical, and the amplitudes of the signal peaks agreed to within 5%. The pulse shape of the emission signal also corresponded to that of the radiation pulse.

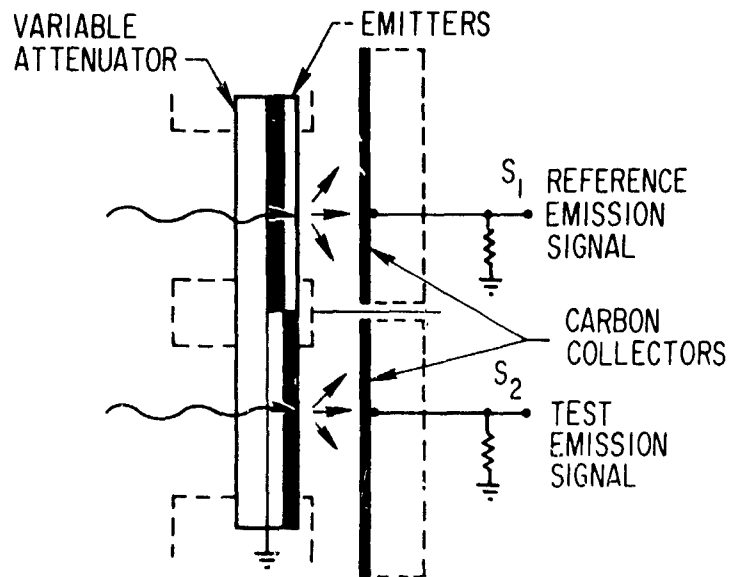
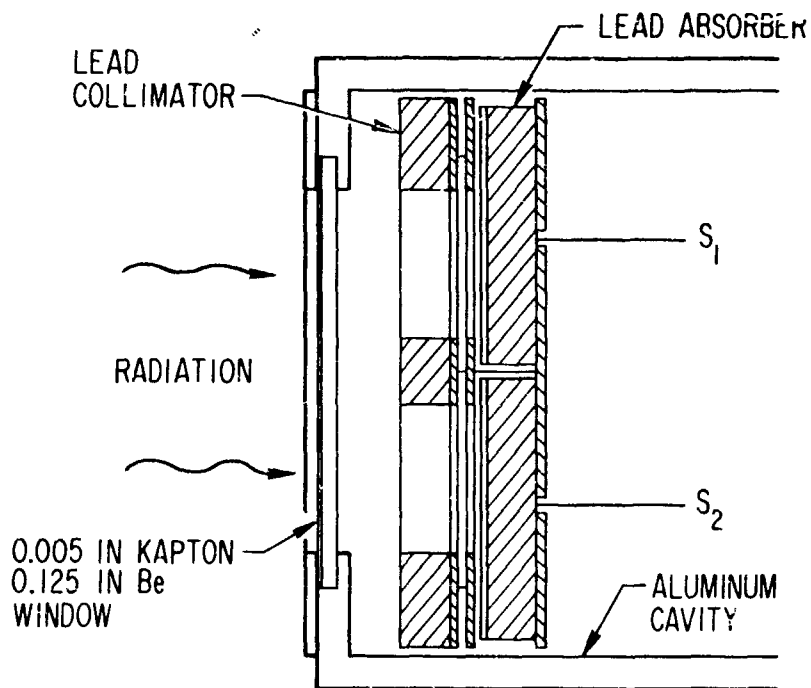


Figure 2. Diagram of the Parallel Diodes  
 a. Experimental arrangement.  
 b. Details of the emitters and collectors.

Table 1. Parameters in Photoemission from Polymers and Other Materials

Material	Composition	Thickness, cm	$\mu$ (22 keV), $\text{cm}^2/\text{g}$	$E = E_{ph} - E_K$ , keV
Polyethylene (PE)	$\text{C}_4\text{H}_8$	0.0152	0.12	21.7
Kapton	$\text{C}_{22}\text{H}_{10}\text{N}_2\text{O}_5$	0.0128	0.197	21.6
Mylar	$\text{C}_{10}\text{H}_8\text{O}_4$	0.019	0.218	21.5
Teflon	$\text{C}_4\text{F}_8$	0.084	0.505	21.4
Polyvinyl Chloride (PVC)	$\text{C}_4\text{H}_6\text{Cl}_2$	0.0715	3.01	19.3
Saran	$\text{C}_4\text{H}_5\text{Cl}_3$	0.0013	3.51	19.2
Mica	11.8% $\text{K}_2\text{O}$ , 38.5% $\text{Al}_2\text{O}_3$ 45.2% $\text{SiO}_2$ , 4.5% $\text{H}_2\text{O}$	0.0051	1.85	20.6
Glass	72% $\text{SiO}_2$ , 15% $\text{Na}_2\text{O}$ 9% $\text{CaO}$ , 3% $\text{MgO}$ , 1% $\text{Al}_2\text{O}_3$	0.0835	1.92	19.3
Carbon	C	0.152	0.14	21.7
Aluminum	Al	0.0025	2.2	20.4
Copper	Cu	0.0046	24.0	13.1
Tantalum	Ta	0.00051	46.0	11.1 ( $E_{ph} - E_L$ )

The effect of low energy secondary electron emission was determined by biasing one diode at a potential that was varied from +280 V to -280 V while the other diode remained unbiased. Electrostatic shielding prevented the applied bias field from penetrating the unbiased unit. The normalized results are given in Fig. 3 for emitters of PVC and of aluminum. The ratio of the biased to unbiased emission signals is denoted by  $S/S_0$ , where  $\kappa_+$  and  $\kappa_-$  are the values of this ratio at large positive and negative biases, respectively. It is shown in the analysis that the contribution of secondary electrons to the observed signal in the unbiased diode can be estimated from these data.

With both diodes unbiased, the relative emission was determined for the various materials, as shown in Fig. 4. The data have been normalized to emission from aluminum and plotted as a function of the photoelectric absorption coefficient  $\mu$  of the material (Ref. 4). Each data point represents the average of at least three normalized signals, and the data bar indicates the full spread in the values of these signals. These results show that the observed emission is proportional to  $\mu$  to a high approximation, for the polymers as well as for the other materials. But the data for copper and tantalum show substantial deviations from emission proportional to  $\mu$ , a result attributed to the relatively large K and L shell binding energies of these metals, as explained in the analysis.

An estimate of the absolute magnitude of photoemission from the various materials is obtained from Fig. 4 by specifying the measured photocurrent density from aluminum. On a typical discharge, the peak current density was  $0.37 \text{ mA/cm}^2$  and the corresponding radiation intensity at the aluminum emitting surface was  $9.7 \times 10^3 \text{ cal/sec-cm}^2$ . This latter intensity was obtained from the PIN silicon detector signal, taking into account the spectral distribution shown in Fig. 1. For comparison with published values of quantum yield, a mean photon energy of 22 keV is assumed for the incident radiation, giving a peak photon flux of  $1.1 \times 10^{19} \text{ photons/sec-cm}^2$ . These values give a quantum yield of  $2.1 \times 10^{-4} \text{ electron/photon}$ , which is consistent

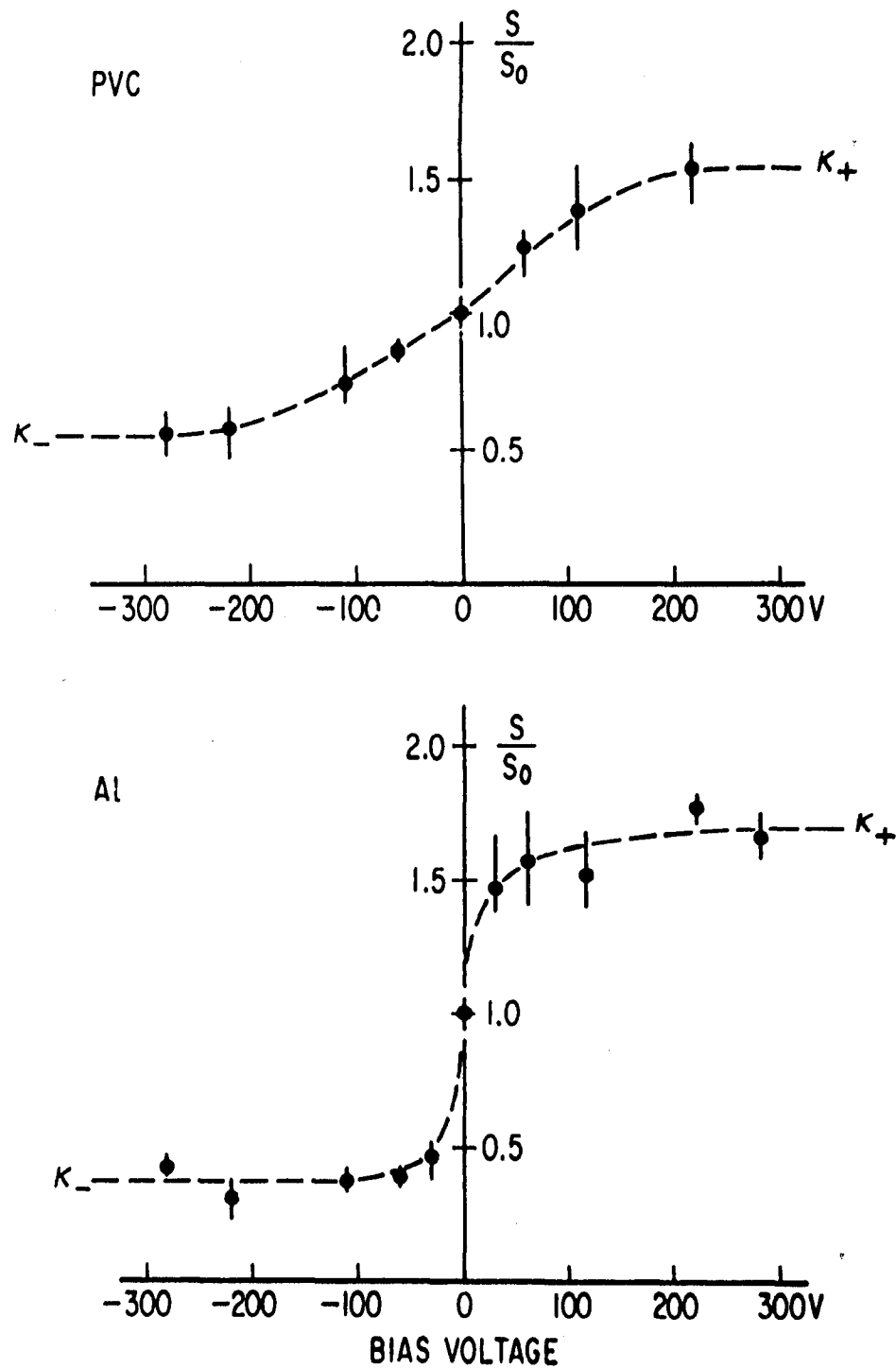


Figure 3. Ratio of Biased Diode Signal to Unbiased Diode Signal as a Function of Bias Voltage for PVC and Aluminum

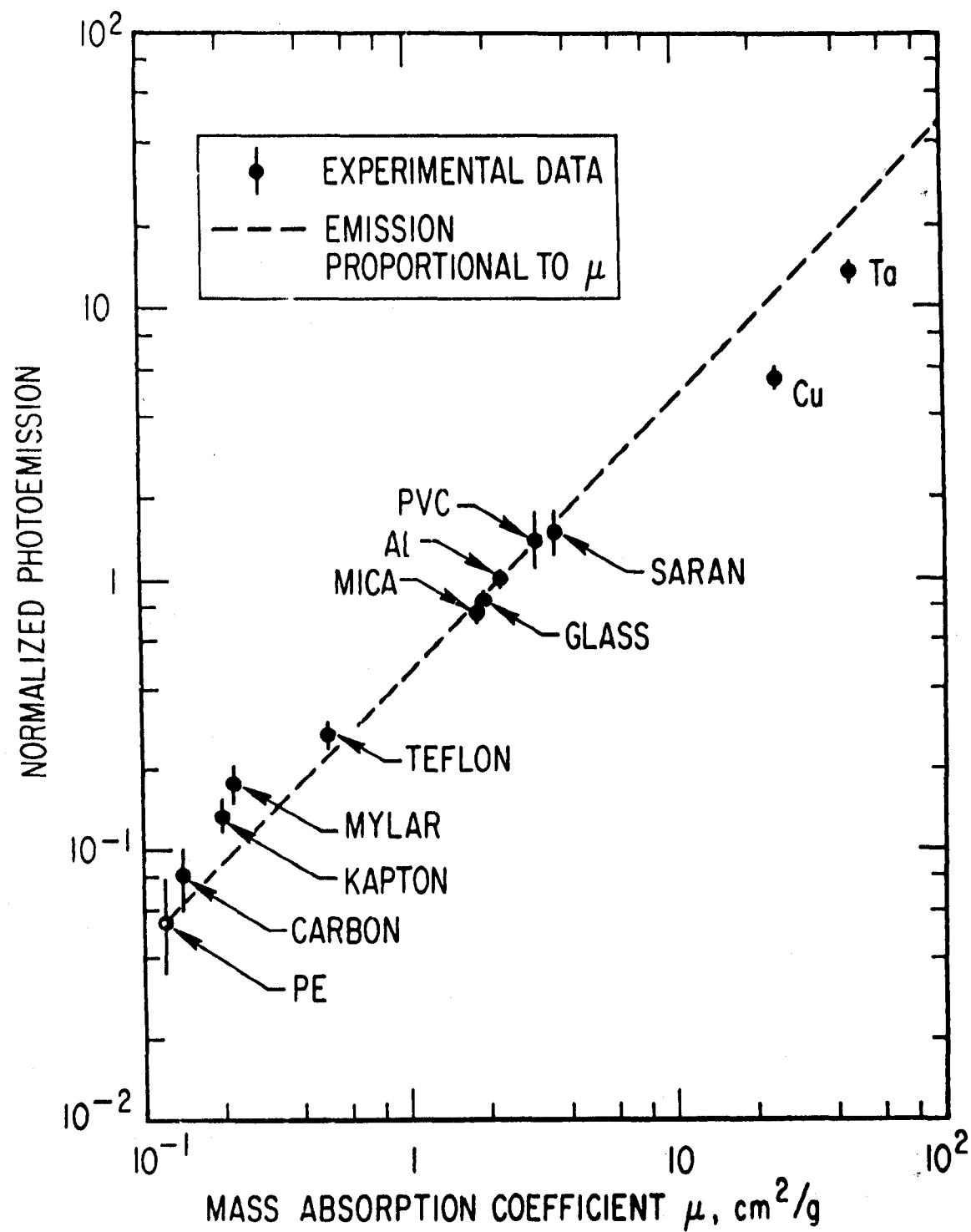


Figure 4. Variation of Normalized Photoemission with the Mass Absorption Coefficient at 22 keV for Various Materials



with the value  $1.3 \times 10^{-3}$  corrected for non-normal incident photon flux and obtained with lower-energy 8 keV photons as given in Ref. 1.

In the measurements described above, insulators backed by a grounded conducting sheet gave emission signals that were identical in shape to those from the reference aluminum conductor. But insulators without this conductive backing were observed to give nonidentical signals. This important variation was examined with the aid of the dual diodes, each with a PVC emitter, one backed by a sheet of aluminum as before and the other isolated. Several discharges were fired with both diode collectors unbiased. The pulse shape of the signal from the isolated PVC was somewhat erratic when compared to that from the grounded PVC, particularly on the first few discharges, one of which is shown in Fig. 5a. (Both PVC emitters had been irradiated a few days before.) After several discharges, however, the pulse shapes were generally similar, but the amplitude of the signal from the isolated sheet was only 30 to 60% of that from the grounded sheet of PVC. Even with both diodes biased at +280 V, the amplitude of the emission signal from the isolated sheet was significantly smaller than that from the grounded sheet, as shown in Fig. 5b. However, when the bias was removed from both diodes, the signal from the isolated sheet again exhibited an anomalous pulse shape similar to that observed when the sheet was first irradiated, as shown in Fig. 5c. After several more discharges, the signal pulse reverted to its usual character, i.e., lower pulse height and similar pulse shape, as shown in Fig. 5d. These variations can be explained on the basis of induced charges in the conductor backing the PVC and of volume and surface trapped charges in the isolated PVC, as discussed below.

TIME SCALE 100 nsec/DIV

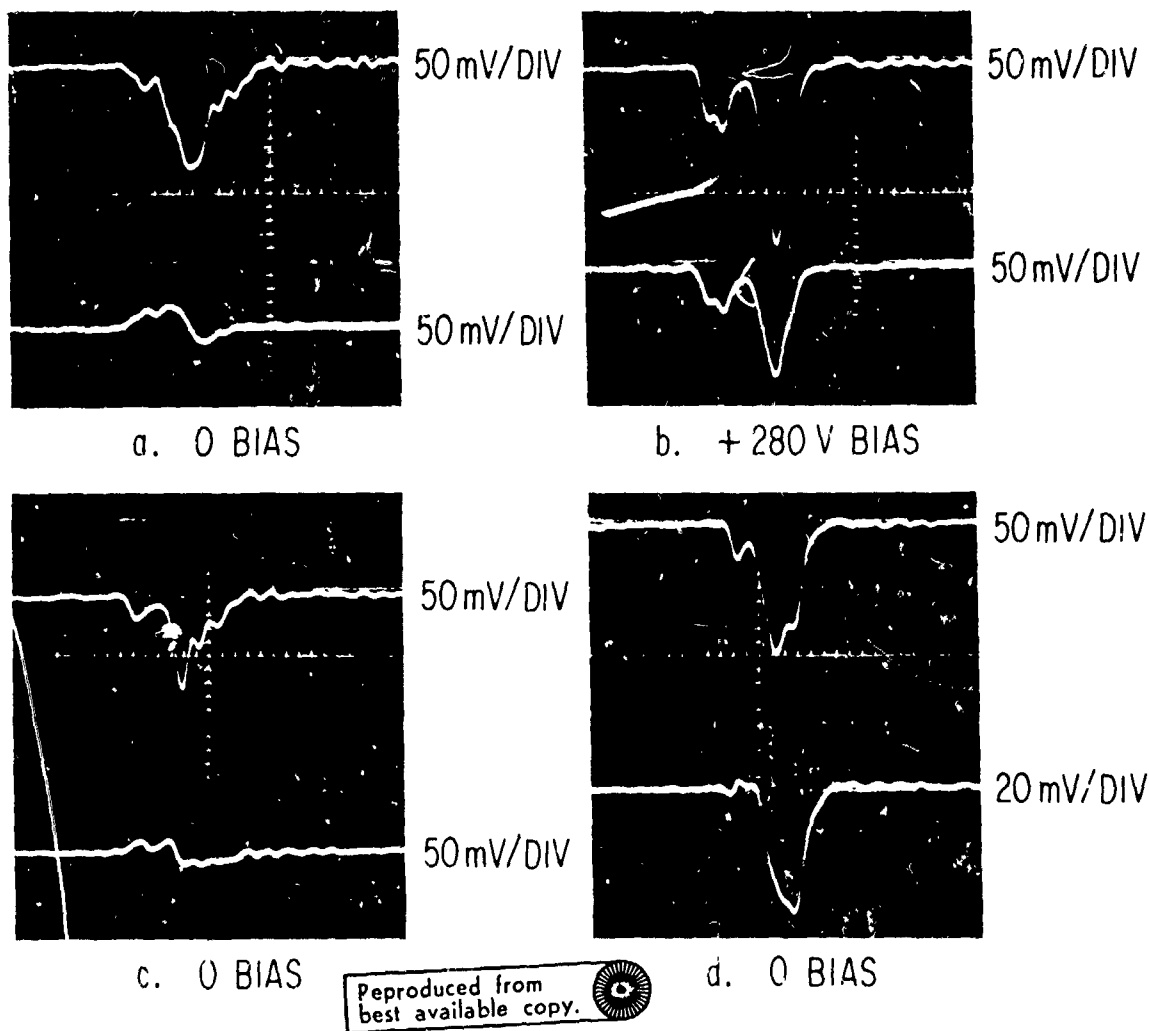


Figure 5. Emission Signals from PVC Observed on the Diode Collectors

Upper trace - grounded PVC emitter; lower trace - floating PVC emitter. a. Initial signals at 0 bias. b. Signals with +280 V bias on both collectors. c. Signals at 0 bias immediately after several irradiations at positive bias. d. Signals at 0 bias after many irradiations.

### III. ANALYSIS

Various theories requiring computer solutions have been generated to describe photoemission from solids. These analyses take into consideration such processes as photoelectric, Compton, Auger, fluorescent, and secondary electron emissions. Because the emitters of primary interest are of rather low atomic number  $Z$  and the photons are sufficiently low in energy, the only processes considered in this report will be photoelectric and secondary electron emissions. Furthermore, because the measured relative emission is observed to closely follow the photoelectric absorption coefficient, a simple analysis of photoelectric emission is first described and correlated with the experimental measurements given in Fig. 4.

In this analysis, photoelectric emission  $\epsilon_P$  from the rear surface of an irradiated sheet is given by

$$\epsilon_P = N_0 (e^{\rho\mu R} - 1) \approx N_0 \rho\mu R \quad (1)$$

where  $N_0$  is the photon fluence at the emitting surface,  $\rho$  is the density of the material,  $\mu$  is the photoelectric absorption coefficient, and  $R$  is the range of the emitted electrons in the material. Kusnezov has shown for several metals that forward photoelectric emission exceeds backward emission (Ref. 5). Therefore, the backward photoelectric emission from the low  $Z$  carbon is assumed to be negligible when compared to forward emission from the high  $Z$  materials. However, this backward emission should be considered when examining emission from the low  $Z$  materials.

The range  $R$  in Eq. (1) is dependent on the electron energy  $E$ , which is equal to the incident photon energy  $E_{ph}$  minus the  $K$  shell binding energy  $E_K$ . (L and M shell binding energies are considered when necessary.) The range  $R$  of kilovolt electrons is approximately described by

$$R = (k/\rho) E^n \quad (2)$$

where  $k$  and  $n$  are constants, usually determined empirically for a specific material and in a particular electron energy interval. Several theoretical and experimental efforts to relate  $k$  and  $n$  to constants of the material have been reported (Refs. 6 and 7). However, these have been limited to metals and metallic compounds and have given results that were not always in agreement with one another. Berger and Seltzer have computed electron ranges for various materials, including those for several polymers (Ref. 8). Some of their results for the 10 to 40 keV range, extrapolated to 1 keV for convenience in obtaining  $k$ , are shown in Fig. 6. Values of both  $k$  and  $n$  are easily obtained from this graph, where  $R' = \rho R$  has been plotted as a function of electron energy. Equations (1) and (2) show that  $\epsilon_p$  is independent of density and depends only on  $\mu$  and  $k'$ .

Absolute values of photoemission computed from Eq. (1) with electron ranges obtained from Fig. 6 are only order of magnitude approximations, because this simple analysis has neglected angular emission and multiple scattering. Photoelectrons are generated in the material with an angular distribution dependent primarily on incident photon energy. These electrons then undergo multiple scattering, which results in nonlinear trajectories. The data given in Fig. 6 describe the mean lengths of these nonlinear trajectories. Therefore, direct application of Eq. (1) requires correction of the electron range data in Fig. 6 by taking into account these factors. These corrections, in general, do not heavily depend on the emission material, e.g., the result of multiple scattering is a reduction in the mean trajectory length based on statistical variations. Thus, these factors tend to cancel in ratios of emissivities, and relative emission is fairly well described by taking the ratios of Eq. (1).

The quantity that has been directly observed is relative emission. From Eqs. (1) and (2), the relative photoemission is given by

$$S_0(\text{mat})/S_0(\text{Al}) = [\mu(\text{mat})/\mu(\text{Al})] \times [k(\text{mat})/k(\text{Al})] [E^n(\text{mat})/E^n(\text{Al})] \quad (3)$$

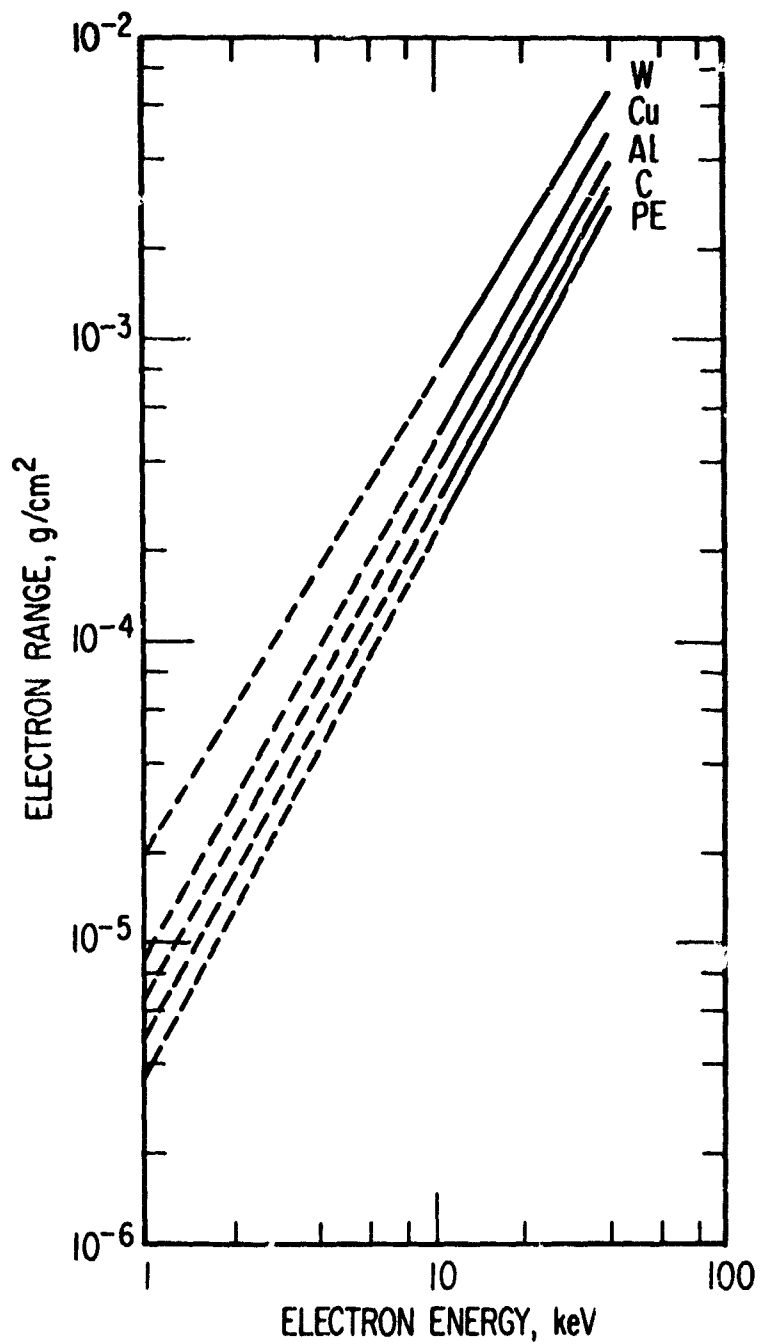


Figure 6. Variation of Electron Range with Electron Energy  
Curves based on tabulation given in Ref. 8 for  
energies in the range 10 - 40 keV.

The variation of each of the bracketed factors on the right in Eq. (3) is examined first for materials listed in Table 1 in which the average binding energy is small, i.e., all the materials except for Cu and Ta. In this group,  $E(\text{mat})/E(\text{Al}) \approx 1$  to within 6% and  $n \approx 1.75$  as suggested by Fig. 6. Also from Fig. 6,  $0.7 \leq k(\text{mat})/k(\text{Al}) \leq 1$ , except for PE. These two terms together, therefore, produce a maximum variation of  $\leq 20\%$ , again excluding PE. The term  $\mu(\text{mat})/\mu(\text{Al})$  varies from 0.055 to 1.6, changing by more than an order of magnitude. Thus, the relative photoelectric emission for this group of materials is dependent primarily on the mass absorption coefficient as observed in the experimental data shown in Fig. 4.

In Cu and Ta, the shell binding energies are no longer small, so that  $E(\text{mat})/E(\text{Al}) < 1$ . In order to compare analysis with experiment, all three terms in Eq. (3) must be evaluated for these two metals. For Cu,  $kE^n(\text{Cu})/kE^n(\text{Al}) = 0.58$ , with  $k$  and  $n$  obtained from Fig. 6. Insertion into Eq. (3) gives  $S_0(\text{Cu})/S_0(\text{Al}) = 6.3$ , a result that is in reasonable agreement with the observed value of 5.5. For Ta, the assumed incident photon energy is smaller than the K shell energy, so that it is necessary to consider the L shell energy. Use of  $k$  and  $n$  obtained from the curve for W in Fig. 6, with  $E = E_{\text{ph}} - E_L$ , gives  $S_0(\text{Ta})/S_0(\text{Al}) = 15.7$ , which is just above the observed value of 13.5.

The contribution of secondary electrons to the observed emission has been assumed to be negligible. This assumption is examined in the following analysis. In a diode configuration, passage of kilovolt photoelectric electrons through the thin layer of thickness  $\Delta x$  ( $\Delta x \ll R'$ ) at the emitter surface generates low energy ( $\leq 50$  eV) secondary electrons, which can escape from the material along with the high energy primary electrons. Furthermore, impact of these primary electrons on the collector surface also generates secondary electrons. The number of escaping secondaries per primary electron is given by the relation  $\delta = (\Delta x/\epsilon) dE/dx$ , where  $\Delta x$  is the mean escape depth,  $\epsilon$  is the average energy to produce one secondary, and  $dE/dx$  is the collisional stopping power. This type of secondary emission from metals has recently been examined by Burke, Wall, and Frederickson (Ref. 9).

Consideration of only forward photoelectric emission but both forward and backward secondary emissions yields

$$S_0 = \epsilon_P (1 + \delta_E - \delta_C) \quad (4)$$

where  $S_0$  is the signal observed on the unbiased collector,  $\epsilon_P$  is the photoelectric contribution,  $\delta_E \epsilon_P$  is the contribution of secondaries from the emitter, and  $\delta_C \epsilon_P$  is that from the collector. An estimate of the net secondary contribution is obtained by examining the emission signals at large positive and negative potential biases, as described in Section II. For a positive bias,  $S_+ = \epsilon_P (1 + \delta_E)$ , and for a negative bias,  $S_- = \epsilon_P (1 - \delta_C)$ . The experimentally observed quantities at large positive and negative biases are  $S_+/S_0 = \kappa_+$  and  $S_-/S_0 = \kappa_-$ . From these equations, the contribution from secondaries with no bias on the collector is given by

$$\Delta\epsilon_S = \epsilon_P (\delta_E - \delta_C)/S_0 = 2 - \kappa_+ - \kappa_- \quad (5)$$

and the ratio of secondaries from the emitter to those from the carbon collector is given by

$$\Gamma_S = \delta_E/\delta_C = (1 - \kappa_-)/(\kappa_+ - 1) \quad (6)$$

From Fig. 3 for PVC,  $\kappa_+ = 1.53$  and  $\kappa_- = 0.55$ , so that  $\Delta\epsilon_S = 0.08$  and  $\Gamma_S = 0.85$ . For aluminum,  $\kappa_+ = 1.7$ ,  $\kappa_- = 0.4$ ,  $\Delta\epsilon_S = -0.10$ , and  $\Gamma_S = 0.86$ .  $\kappa_+$  and  $\kappa_-$  have also been measured for mylar, copper, and tantalum; the results for these materials are given in Table 2.

Table 2. Biased Diode Parameters

Type	$\kappa_+$	$\kappa_-$	$\Delta\epsilon_S$	$\Gamma_S$
Mylar	1.9	-0.3	0.4	1.45
PVC	1.53	0.55	-0.08	0.85
Al	1.7	0.4	-0.10	0.86
Cu	1.7	0.5	-0.20	0.71
Ta	2.0	0.5	-0.50	0.50

The shape of the bias curve for mylar was similar to that observed for PVC in Fig. 3, and those for copper and tantalum were similar to the one for aluminum. The results in Table 2 indicate that secondary emission from the carbon collector exceeded that from the emitter for all the materials except mylar. The net contribution of secondaries was relatively small for PVC and aluminum but was larger for mylar, copper, and tantalum.

The correction for secondary emission  $[1 - \Delta\epsilon_s(\text{mat})]/[1 - \Delta\epsilon_s(\text{Al})]$ , giving relative photoelectric emission, would change the observed value in Fig. 4 for Cu to 6.0 (predicted value 6.3) and for Ta to 18.4 (predicted value 15.7). Also, this correction would leave the value for PVC almost unchanged but would reduce that for mylar to 0.096, a value closer to that given by emission proportional to  $\mu$ , as indicated in Fig. 4. Consideration of backward photoelectric emission, in addition, would only slightly increase this value.

The effect of a positive charge layer produced by photoemission on subsequent emission from polymers and other insulators has also been neglected. Observations described in the preceding section have shown that emission depended on whether the emitting polymer sheet was isolated or backed by a grounded conducting sheet. The relation of a charge layer to these observations is examined by computing the energy required for an electron to cross the emitter-collector gap shown in Fig. 2, first for a monopole layer emitter and then for a dipole layer emitter. The emitter configuration assumed is a uniformly charged disk of radius  $A$  ( $A = 1.43$  cm), and electron emission from the center of this disk is examined. The perturbative effects of the dielectric properties of the emitter and of the grounded collector are neglected. The monopole layer emitter corresponds to the charge configuration produced by emission from an isolated sheet of polymer. The required energy  $U$  in this configuration is given by

$$U = (\sigma/2\epsilon_0) d (1 - d/2A) \quad (7)$$



where  $\sigma$  is the layer charge density,  $\epsilon_0$  is space permittivity, and  $d$  is the gap separation. For PVC, a reasonable charge density is  $\sigma = 3.7 \times 10^{-11} \text{ C/cm}^2$  (produced by a 100 nsec pulse of magnitude given above for aluminum), and  $d = 3 \times 10^{-1} \text{ cm}$ . Equation (7) yields  $U \approx 57 \text{ eV}$ . Thus, the low energy secondary electrons but not the high energy photoelectrons are easily prevented from crossing the gap. In addition, the electric field of this monopole layer increases secondary emission from the collector.

The dipole layer emitter corresponds to the charge configuration produced by photoemission from a sheet of polymer backed by a grounded conducting sheet, the negatively charged layer being that induced on the surface of the grounded conductor. The required energy in this case is

$$U \approx (\sigma/2\epsilon_0) (d t/A) \quad (8)$$

where  $t$  is the dipole layer separation. For the same charge density given above and  $t = 7.2 \times 10^{-2} \text{ cm}$ , thickness of the PVC sheet, the required electron energy is only 0.31 eV. Therefore, use of a conductive backing in emission from sheets of polymers can greatly reduce the retardation of the low energy secondaries produced by photoemission, giving the results described in the preceding section.

For a low  $Z$  polymer and an aluminum backing, a net negative charge is deposited in the polymer. This photoelectric emission, in effect, reduces the charge density of the dipole sheet, which further decreases the required energy.

#### IV. DISCUSSION AND CONCLUSION

The two main results derived from this investigation are: (1) the relative magnitudes of photoemission from many materials, both insulators and conductors, are proportional mainly to the values of the mass absorption coefficients; and (2) the emission from an isolated insulator differs substantially from emission from an insulator in close contact with a grounded conductor. The conditions under which these two results are valid are discussed below.

The observed dependence on  $\mu$  requires the energy of the emitted electrons in the material to be approximately that of the similarly emitted electrons in aluminum, an energy that is slightly less than the incident photon energy. This condition is met for most of the materials listed in Table 1 but not for the two high Z metals because of large shell binding energies, and here significant deviations from this  $\mu$  dependence occur. The dependence also requires a fortuitous cancellation of the contributions from secondary electrons from the emitter and collector in order that the observed emission is mainly photoelectric emission. Cancellation of the very low energy but not the high energy secondaries is produced by the retarding potential of the space charge in the emitter-collector gap during emission. But the results of studies of the variation of emission with bias indicate that total cancellation does not occur for many of the materials. However, even with correction for this noncancellation of secondaries based on the bias measurements, this  $\mu$  dependence is still evident.

In the experimental determination of relative emission, the insulators were always backed by grounded conducting sheets. Use of these sheets prevented varying signals and produced fairly reproducible emission over several discharges. The explanation for this observation, supported by the analysis of the dipole layer, is that negative charges are induced in the grounded conducting sheet and nullify the field effect of trapped positive charges formed by ejection of photoelectrons from the insulator, thereby greatly reducing the electric field between the emitter and collector.

The second result listed above is based on observations such as those shown in Fig. 5. The explanation proposed is that, whereas an insulator backed by a grounded sheet has the aid of induced charges to help stabilize its emission, the isolated sheet of insulator must rely on the accumulation of negative surface charge to nullify the effect of the trapped positive volume charge. When this surface charge has been removed, either by handling before initial irradiation or by an applied field during irradiation, fields produced by the trapped positive charge tend to reform a surface charge through retardation of secondary emission from the insulator and attraction of electrons emitted from other surfaces. This interaction can result in signals such as those shown in Fig. 5a and 5c. After accumulation of sufficient surface charge, emission from the isolated insulator is semi-stabilized (Fig. 5d).

In the above discussions, a definite distinction has been made between secondary and photoelectric electrons. This separation of the two species may be easily performed experimentally for metals through application of a bias. This effect is shown in the bias curve for aluminum in Fig. 3, in which the collector signal changed from maximum to minimum value over a very narrow range of bias voltage, from +30 to -30 V. Outside this range, the signals are relatively constant, clearly establishing saturation values  $\kappa_+$  and  $\kappa_-$  used in the estimation of the secondary electron contribution. Examination of the bias curve for PVC in Fig. 3 does not show this large change in signal over a small range of bias voltage, thus indicating that there is no distinct division between low energy secondaries and high energy photoelectrons for the polymer. In addition, the signals within the indicated range of bias voltages do not attain clearly defined saturation values, particularly at large positive biases. (This variation was also observed for mylar.) This continued increase in signal with positive bias may be partially produced by the bulk photoconductivity. Thus, the secondary electron contributions for the polymers based on the values given for  $\kappa_+$  and  $\kappa_-$  are only rough estimates. These observations imply that the conventional method of

examining high energy emission by placing a small negative bias on a grid placed in front of the collector may not be applicable in the investigation of photoemission from the polymers.

The separation of secondaries from primaries for aluminum has been performed (Ref. 10), and it has shown that there is a distinct secondary electron component with energies below ~100 eV and a photoelectron component that increases monotonically with energy to a maximum at  $E = E_{ph} - E_K$ . An experimental study, similar to this one, examining the energy structure of electron emission from grounded and isolated sheets of polymers would be highly informative with respect to many of the phenomena just described.

## REFERENCES

1. V. N. Shchemlev, L. G. Eliseenko, E. P. Denisov, and M. A. Rumsh, "Current and Pulse Measurements of the X-Ray Photoemission of a Massive Cathode," FFT 6, 2574 (1964) [Soviet Physics - Solid State 6, 2051 (1965)].
2. W. T. Ogier and D. V. Ellis, "Soft X-Ray Photoelectric Yield Formulas," J. Appl. Phys. 36, 3788 (1965).
3. H. L. L. van Paassen, R. H. Vandre, and R. S. White, "X-Ray Spectra from Dense Plasma Focus Devices," Phys. Fluids 13, 2606 (1970).
4. W. H. McMaster, N. Kerr Del Grande, J. H. Mallett, and J. H. Hubbell, Compilation of X-Ray Cross Sections, UCRL 50174 (1969).
5. N. Kusnezov, "Photoelectric Yield," IEEE Trans. Nucl. Sci. NS-17, No. 6, 190 (1970).
6. C. Feldman, "Range of 1-10 keV Electrons in Solids," Phys. Rev. 117, 455 (1960).
7. I. M. Bronshtein and A. N. Brozdnichenko, "Range of Electrons with Energies of .5 to 4 keV in Mg, MgO, BeO, and  $Al_2O_3$ ," FFT 11, 187 (1969) [Soviet Physics - Solid State 11, 140 (1969)].
8. M. J. Berger and S. M. Seltzer, "Tables of Energy-Losses and Ranges of Electrons and Positrons," Studies in Penetration of Charged Particles in Matter, National Research Council, Publication 1133, 205 (1964).
9. E. A. Burke, J. A. Wall, and A. R. Frederickson, "Radiation-Induced Low Energy Emission from Metals," IEEE Trans. Nucl. Sci. NS-17, No. 6, 193 (1970).
10. E. P. Denisov, V. N. Shchemelev, A. N. Mezhevich, and M. A. Rumsh, "Analysis of the Energy Structure of X-Ray Photoemission from a Massive Cathode," FFT 6, 2569 (1964) [Soviet Physics - Solid State 6, 2047 (1965)].

Preceding page blank